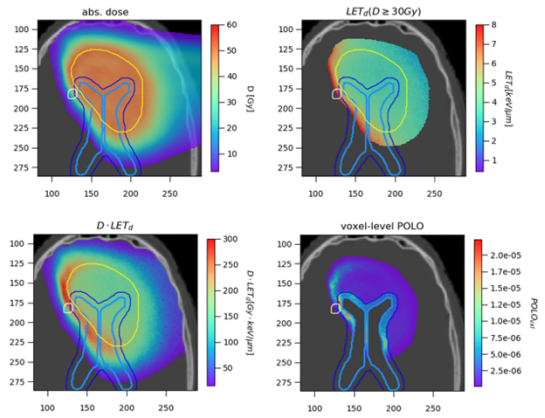

Figure 1: Colourwash overlay of Monte Carlo calculated quantities (a) absorbed dose D (b) dose-averaged LET (LET_d) for voxels receiving at least 30 Gy absorbed dose, (c) the product D·LET_d and (d) the probability of lesion origin (POLO) distribution predicted by the NTCP model, visualised on top of the treatment planning CT image for a patient treated with a two field spot-scanning proton plan. Voxels outside the brain were masked for the overlays (b-d). The clinical target volume is delineated in yellow, the ventricular system in light blue, the ventricular proximity in dark blue and the observed contrast-enhancing brain-lesion in white.

Results

Lateral target volumes, predominantly seen for WHO °II histologies in an old patient group (median age 45 yrs), were identified as unfavourable in terms of VP load, with a median NTCP of 11% (range [0.06,62]%). The comparably young patient group (median age 16 yrs) with WHO °I tumours had mostly central target locations yielding a considerably lower median NTCP of 1% (range [0.06,78]%) (cf Fig. 2). Despite a maximum RBE of ~1.6 extracted at LET_d=5 keV/µm in the patient cohort, the VP was found to be the main driver of high risks. Tested CP strategies were not able to effectively decrease NTCP. In fact, most scenarios yielded an increase due to an unfavourable redistribution of intermediate to high LET_d into the sensitive VP.

RADP succeeded in constraining the NTCP at the cost of some underdosage to the PTV and CTV edges overlapping with the sensitive VP. Depending on the overlap size, local dose reductions of up to 20% were required to achieve NTCP≤10%. As the required dose reduction depends on the local LET_d, intricate patterns of sparing are obtained. Thus, RADP also re-distributes LET_d away from the ventricles to some extent, leading to a small but noticeable reduction of POLO in the entire target volume.

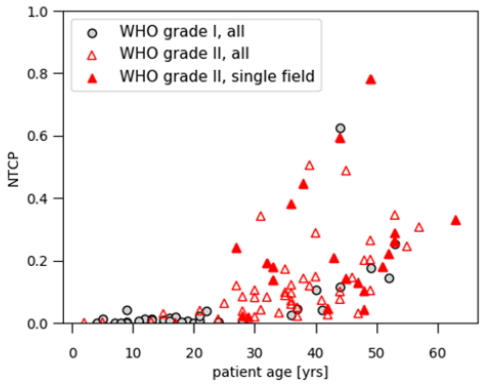

Figure 2: NTCP distribution in the modelling patient cohort as a function of patient age, stratified by the tumour grade, with WHO°I subjects represented by filled grey circles and WHO°II subjects by red triangles. In the latter group, subjects treated with a single field are highlighted by filled red triangles.

Conclusion

An NTCP model comprising a spatially variable radiosensitivity and high-LET_d dependence in dose optimization leads to risk avoiding, patient specific dose and LET_d redistribution in proton treatment of LGG. These effects could not be achieved with CP strategies.

PO-1457 Modified 2D UNet for automatic segmentation of the nasopharyngeal carcinoma on CT images

L. Wu[1], J. Yen[2], J. Lee[3], C. Jen[2], H. Cheng[2], C. Chen[3]
[1]Koo Foundation Sun-Yat-Sen Cancer Center, Medical physics, Taipei City, Taiwan ; [2]Koo Foundation Sun-Yat-Sen Cancer Center, Radiation oncology, Taipei City, Taiwan ; [3]Academia Sinica, Institute of Information Science, Taipei city, Taiwan

Purpose or Objective

Recent advances in deep neural networks (DNNs) have unlocked opportunities for their application of automatic image segmentation. We modify the structure of UNet to become a modified 2D UNet for segmenting the region of nasopharyngeal carcinoma (NPC) on computed tomography (CT) images which were filled with the effect of metal artifacts. We have evaluated and compared the efficacy of several DNN-based algorithms including modified 2D UNet, Deeplabv3, VNet and Deep deconvolutional neural network (DDNN)for automatic segmentation of NPC.

Material and Methods

Planning-CT data sets from 224 patients with NPC were selected. Among these data sets, 184 were used for training, 40 for validation. All images were resampled to a spatial resolution of 1 × 1 × 2.5 or1 × 1 × 3 mm. Several severe denture metal artifacts were observed in 125 images that reflect the real world circumstance. In image preprocessing, we utilized the image enhancing technique to make the soft tissue of CT images to explicit before each voxel value in the images would be normalizedwithin the range of 0 to 1. Data augmentation methods including flip horizontally, rotation, shift, shear, and zoom were used to avoid overfittingin the training model. Our modified 2D UNet is constructed with synchronized batch normalization layers based on the structure of the UNet. After obtaining the outputs of the modified 2D UNet, we utilized the connected component and morphology algorithm to refine it. Results were compared between the outputs of each DNNand physician-generated contours using the3D Dice similarity coefficient (DSC) and the modified average object using the Hausdorff distance (OHD).

Results

Among modified 2D UNet, Deeplabv3, VNet and DDNN-based nasopharyngeal primary tumor(GTVp) and lymph node metastasis (GTVn) segmentation, the modified 2D UNet had the best performance. The 3D DSC for GTVp and GTVn was 72.6% and 70.7%, respectively. The mean OHD for GTVp and GTVn was 13.7mm and 35.4mm, respectively. It took 10 seconds to generate the segmentation for each patient.

Conclusion

The modified 2D UNet has the best performance compared to other DNNs. The accuracy of segmentation was interfered with by severe metal artifacts but improved after standardized the voxel value. Future work will focus on eliminating the effect of metal artifacts by incorporating synthetic CT scans from paired MRI images.

PO-1458 Robust treatment planning for GammaKnife radiosurgery accounting for target contouring uncertainties

H. Sandstrom[1], H. Nordström[2], I. Toma-Dasu[3]
[1]Medical Radiation Physics, Stockholm University, Stockholm, Sweden ; [2]Elekta Instrument AB, Stockholm, Stockholm, Sweden ; [3]Medical radiation physics, Department of Physics- Stockholm University and Oncology & Pathology- Karolinska Institutet, Stockholm, Sweden

Purpose or Objective
One of the key problems in Gamma Knife stereotactic radiosurgery (SRS) is the definition of the target. Previous studies revealed that in spite of high accuracy in delivering the prescribed dose, there is high variability in contouring not only complicated but also common SRS targets. The aim of this study therefore was to develop a robust treatment planning approach for Gamma Knife SRS accounting for uncertainties in target definition.

Material and Methods
Twenty Gamma Knife centres participated in a contouring and planning study for complicated SRS targets (anaplastic astrocytoma, arteriovenous malformation, vestibular schwannoma) and twelve in the study of common targets (cavernous sinus meningioma, vestibular schwannoma, pituitary adenoma and two metastases). The results were analysed with respect to variability in contouring and dose distribution. In order to test the feasibility of a probabilistic planning approach meant to mitigate the uncertainties in target delineation, a robust plan was created for the cavernous sinus meningioma case, chosen among the common targets, incorporating the variability in contouring in the optimization process as weights for the objective function. In addition, optimized plans were created for all individual contours and for the average target volume. Selectivity, coverage, gradient index, V10 and V12 were calculated and compared for all plans and used for the comparison of the nominal and optimized plans together with the beam-on-time and the efficiency index.

Results
The results from the robust treatment planning approach showed that it is feasible to include uncertainties in the extent and position of the target volume and generate an optimized plan taking this into account. A high coverage (96-97%), selectivity (90-93%) and gradient index (2.75-2.94) was obtained for all optimized plans for individual contours as well as for the robust plan (coverage 93-97%, selectivity 73-86%). Comparison of the nominal and optimized plans showed higher coverage and selectivity for the later, at the same time as the beam-on-time decreased. V12 and V10 are below recommended limits and lower for the optimized plans (V12: 7.3-9.3 cm^3, V10: 9.5-12.6 cm^3) compared to the nominal plans (V12: 6.7-12.4 cm^3, V10: 8.7-16.1 cm^3).

Conclusion
The inconsistencies in the variability in contouring translate into differences between dose distributions which could be mitigated through probabilistic robust planning

PO-1459 Fully automated machine learning optimization VMAT planning for oropharyngeal cancer

I. Van Bruggen[1], R. Kierkels[1], M. Holmström[2], H. Gruselius[2], D. Lidberg[2], K. Berggren[2], S. Both[1], J. Langendijk[1], F. Löfman[2], E. Korevaar[1]
[1]UMCG, Radiotherapy, Groningen, The Netherlands ;
[2]RaySearch Laboratories, Machine learning, Stockholm, Sweden

Purpose or Objective
To demonstrate that fully automated volumetric modulated arc therapy (VMAT) dose distributions for oropharyngeal cancer patients can be generated with machine learning optimization (MLO) planning, with similar quality as the clinical 'dosimetrists-optimized' dose distributions, further indicated as reference plans.

Material and Methods
MLO planning involved training of a model using 60 oropharyngeal cancer patients, which was used to predict the voxel dose for new patients. CT scans, structures and dose distributions of 99 consecutive primary oropharyngeal cancer patients, previously treated with dual arc VMAT, were retrieved from our clinical database. Image and contour features were extracted and atlas regression forests (ARF), prediction random forests (pRF) and conditional random fields (CRF) were trained. Using the trained model, spatial dose distributions were predicted and optimized to generate clinical treatment plans while adhering to the predicted dose. Validation was performed with 39 oropharyngeal cancer patients to tune model settings using both target and organ at risk (OAR) quality measures. Clinical machine learning plans and reference plans were compared by means of adequate target coverage (D_{98}≥95%), dose on OARs ($D_{0.1}$, D_{mean}), normal tissue complication probability (NTCP) values (xerostomia, dysphagia and tube feeding dependence) and planning time. Two-tailed p-values were calculated by a paired Wilcoxon signed-rank test and a Bonferroni correction (α=0.05).

Results
The predicted dose was in agreement with the reference dose for all plans, see table 1. Validation showed that it was possible to incorporate clinical requirements in the model settings. In the final settings, both the clinical machine learning and reference plans had adequate target coverage in 37/39 (95%) and acceptable maximum OARs dose in 38/39 (97%) of the plans. The average sum NTCP was 84.5% (±17.8) and 84.9% (±19.4) for clinical machine learning plans and reference plans, respectively. Planning time for reference plans took around 240 minutes and clinical machine learning plans were generated in 65 minutes (±11.2), with negligible hands-on time. Figure 1 shows the average dose volume histogram (DVH) of all reference and clinical machine learning plans.

Table 1 Average results and standard deviation of evaluation on dosimetric parameters, HI, CI and NTCP values of reference, predicted and clinical machine learning plans

	Parameters	Reference plans	Predicted machine learning plans	Clinical machine learning plans
Target coverage	PTV 7000 D_{98} (cGy)	6737 ± 37	6766 ± 32	6745 ± 28
	PTV 7000 D_{mean}(cGy)	7010 ± 27	6983 ± 11	**6983 ± 15***
	PTV 7000 D_2 (cGy)	7238 ± 89	7204 ± 33	**7156 ± 23***
	PTV 7000-1mm $D_{99.9}$ (cGy)	6646 ± 127	6723 ± 38	6698 ± 36
	PTV 7000 HI	0.080 ± 0.03	0.073 ± 0.1	**0.067 ± 0.04***
	PTV 5425 D_{98} (cGy)	5243 ± 41	5276 ± 31	5226 ± 31
	PTV 5425-PTV 7000 D_2 (cGy)	5922 ±112	5771 ± 94	**6097 ± 118***
	PTV 5425-1mm $D_{99.9}$ (cGy)	5144 ± 88	5209 ± 59	**5084 ± 76***
	PTV 5425 HI	0.345 ± 0.026	0.335 ± 0.025	**0.335 ± 0.025***
$OARD_{0.1}$ (cGy)	Brain	3013 ± 1122	2710 ± 751	**2769 ± 1149***
	Brainstem	3380 ± 1067	3146 ± 467	3172 ± 1183
	Spinal cord	4265 ± 382	4085 ± 253	**4804 ± 485***
	Eyes anterior	219 ± 200	109 ± 75.0	224 ± 261
	Eyes posterior	259 ± 213	157 ± 98.0	305 ± 417
OAR mean dose (cGy)	Parotid glands	2584 ± 836	1817 ±798	**2428 ± 812***
	Submandibular glands	5785 ± 1239	5720 ± 1063	5914 ± 1029
	Oral cavity	4691 ± 992	4384 ± 90 1	4573 ± 906
	PCM superior	5824 ± 904	5631 ± 816	**5992 ± 716***
	PCM medius	5509 ± 1008	5134 ± 1016	**5868 ± 660***
	PCM inferior	4068 ± 1239	3725 ± 1113	4224 ± 1062
	Cricopharyngeal muscle	3142 ± 1047	2603 ± 675	3373 ± 791
	Supraglottic	4946 ± 1239	4586 ± 1232	**5257 ± 982***
	Glottic	3662 ± 1340	2909 ± 1126	4160 ± 976
	Thyroid	5109 ± 480	4934 ± 492	5152 ± 411
NTCP (%)	Xerostomia	39.3 ± 6.2	30.7 ± 4.2	**37.7 ± 5.7***
	Dysphagia	32.0 ± 8.5	29.4 ± 7.7	32.2 ± 8.5
	PEG	14.5 ± 5.1	10.9 ± 3.7	**14.9 ± 4.6***
	Sum NTCP	84.9 ± 19.4	70.7 ± 15.2	84.5 ± 17.8
Plan evaluation	PTV 7000 CI95%	0.818 ± 0.038	0.850 ± 0.040	0.818 ± 0.038
	PTV 5425 CI95%	0.826±0.067	0.857 ± 0.054	0.823 ± 0.060
	Monitor units (#)	349 ± 98.5	-	**380 ± 38.8***
	Total planning time (min)	~240	10 ± 5	55 ±10

PTV: Planning Target Volume, HI: Homogeneity Index ((D2-D98)/50), PCM: Pharyngeal Constrictor Muscle, NTCP: Normal Tissue Complication Probability, PEG: Percutaneous Endoscopic Gastrostomy, CI: Conformity Index (TV95/V95)
*Significant difference compared to reference plans

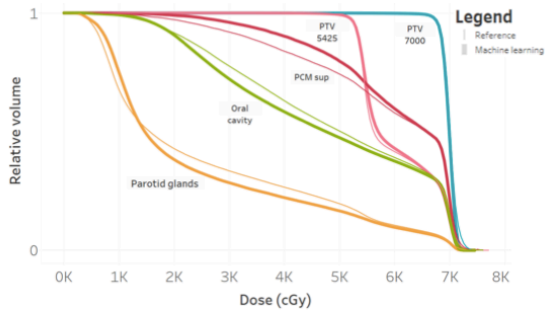

Figure 1 Average dose volume histogram (DVH) of PTV 7000 (blue), PTV 5425 (pink), organs involved in dysphagia: Pharyngeal Constrictor Muscle (PCM) superior (red), oral cavity (green) and organs involved in xerostomia: parotid glands (orange) of 39 oropharyngeal cancer patients of reference (thin lines) and clinical machine learning plans (thick lines).